MOBILITY & VEHICLE MECHANICS

https://doi.org/10.24874/mvm.2024.50.02.04
UDC: 629.1.07

HANDLING AND STABILITY ANALYSIS OF AN AUTOMATED VEHICLE WITH INTEGRATED FOUR-WHEEL INDEPENDENT STEERING (4WIS)

Vasko Changoski[1], Igor Gjurkov[2], Vase Janushevska[3]

Received in July 2024 *Accepted in August 2024*

RESEARCH ARTICLE

ABSTRACT: The latest revisions of the UN and the European Union regulations regarding the steering system allow implementation of novel technologies in automated vehicles. Four-wheel independent steering (4WIS) system represents an upgrade of the steer-by-wire concept that enhances the capabilities of the steering system. The primary focus of this research is to enhance vehicle handling and stability performance by integration of four-wheel independent steering (4WIS) and vehicle stability control (VSC) system in an automated vehicle. A virtual vehicle equipped with 4WIS and VSC is created in ADAMS/Car. The proposed control algorithms are implemented in MATLAB/Simulink and their effect is tested in co-simulation environment. As a control method, Sliding Mode Control (SMC) is used to improve vehicle handling while maintaining vehicle stability under different driving conditions. The proposed concept is evaluated through different open-loop and path following manoeuvres to thoroughly assess its performance.

KEY WORDS: *Four-wheel independent steering (4WIS), steer-by-wire, co-simulation, vehicle handling, vehicle stability.*

[1] *Vasko Changoski, Ss. Cyril and Methodius University in Skopje, Faculty of Mechanical Engineering – Skopje, ul. Rugjer Boshkovikj 18, 1000 Skopje, Republic of North Macedonia, vasko.changoski@mf.edu.mk, https://orcid.org/0000-0001-6148-9389 (*Corresponding author)*
[2] *Igor Gjurkov, Ss. Cyril and Methodius University in Skopje, Faculty of Mechanical Engineering – Skopje, ul. Rugjer Boshkovikj 18, 1000 Skopje, Republic of North Macedonia, igor.gjurkov@mf.edu.mk, https://orcid.org/0000-0001-5887-8797*
3 Vase Janushevska, PhD., Assistant Professor, Ss. Cyril and Methodius University in Skopje, Faculty of Mechanical Engineering – Skopje, ul. Rugjer Boshkovikj 18, 1000 Skopje, Republic of North Macedonia, vase.janushevska@mf.edu.mk, https://orcid.org/0000-0001-5403-3447

ANALIZA UPRAVLJANJA I STABILNOSTI AUTOMATIZOVANOG VOZILA SA INTEGRISANIM NEZAVISNIM UPRAVLJANJEM NA SVA ČETIRI TOČKA (4WIS)

REZIME: Najnovije revizije propisa UN i Evropske unije u vezi sa sistemom upravljanja omogućavaju implementaciju novih tehnologija u automatizovana vozila. Sistem nezavisnog upravljanja na četiri točka (4VIS) predstavlja nadogradnju koncepta upravljanja po žici koji poboljšava mogućnosti upravljačkog sistema. Primarni fokus ovog istraživanja je poboljšanje performansi upravljanja vozilom i stabilnosti integracijom nezavisnog upravljanja na sva četiri točka (4VIS) i sistema kontrole stabilnosti vozila (VSC) u automatizovano vozilo. Virtuelno vozilo opremljeno 4VIS i VSC je kreirano u ADAMS/Car. Predloženi kontrolni algoritmi su implementirani u MATLAB/Simulink i njihov efekat je testiran u ko-simulacionom okruženju. Kao metoda kontrole, kontrola kliznog režima (SMC) se koristi za poboljšanje upravljanja vozilom uz održavanje stabilnosti vozila u različitim uslovima vožnje. Predloženi koncept se procenjuje kroz različite manevre u otvorenom krugu i praćenju putanje kako bi se temeljno procenio njegov učinak.

KLJUČNE REČI: *Nezavisno upravljanje na četiri točka (4VIS), upravljanje po žici, kosimulacija, upravljanje vozilom, stabilnost vozila.*

HANDLING AND STABILITY ANALYSIS OF AN AUTOMATED VEHICLE WITH INTEGRATED FOUR-WHEEL INDEPENDENT STEERING (4WIS)

Vasko Changoski, Igor Gjurkov, Vase Janushevska

INTRODUCTION

Vehicle handling and stability is significantly improving with the advancement of vehicle automated systems. The introduction of active steering systems compared to the traditional front wheel steering system offers improved manoeuvrability but also can improve vehicle stability by correcting driver's commands. With the implementation of the Active Front Steering (AFS) system, a correction on the driver's input is made by adding or subtracting front wheel steering angle [22]. The AFS system could be further improved by applying steer-by-wire system. With the latest revision of the UN regulation ECE – R79 [18], a steer-by-wire concept can be implemented in the new vehicles. This would allow enhanced vehicle control and adaptability of the steering system. Steer-by-wire AFS system is analysed in [21] where a Sliding Mode Control (SMC) is applied in combination with Extreme Machine Learning that results in improved vehicle stability. Shuai et al. in [15] analyse integrated AFS steer-by-wire and direct yaw control (DYC) systems. The results are verified using co-simulation environment between MATLAB/Simulink and Carsim. AFS and DYC are used for integrated vehicle dynamic control with Sliding Mode Control (SMC) where the system demonstrates strong robustness against uncertainties but also improves the transient response of the control system [12].

Another approach in implementation of active steering system, but in this case using four wheels steering (4WS) system and integrated with DYC, is presented in [7] where a linear parameter varying (LPV) system and H∞ optimal control theory are applied to improve vehicle stability. A comparison between vehicle equipped with vehicle stability system (VSC), vehicle with VSC and AFS and vehicle VSC and ARS systems is conducted in [1] where the 4WS vehicle shows greater vehicle stability and handling over the other vehicles. Further improvement in the steer-by-wire system represents the four-wheel independent steering (4WIS) system. Chen et al. suggest using SMC for tracking reference parameters by switching between front wheel steering, rear wheel steering and 4WIS [4]. Researchers in [3] apply Linear Quadratic Regulator (LQR) for coordinated control of 4WIS and four-wheel independent drive (4WID) vehicle for enhanced vehicle stability. Liang et al. suggest using SMC 4WID/4WIS vehicle to improve vehicle stability in high-speed conditions [11]. The authors implement SMC controllers for 4WIS system and SMC controller for yaw corrective moment in combination with phase-plane method (β-$\dot{\beta}$) where a transition between the handling orientated control and stability orientated control is suggested based on the vehicle stability region. Yim and Jo compare different integration combination of AFS, ARS and ESC systems under force constraint of AFS system [20]. The systems are activated in different combination based on the tire side slip angle.

Another aspect of applying 4WIS steering is to improve vehicle path following control. Hang et al. in [6] use Model Predictive Control (MPC) for improved path following in 4WIS vehicle. The MPC controller is applied to control the four wheels steering angles and to apply corrective yaw moment. On the other hand, a combination of Linear Parameter Varying and H∞ controllers is applied in 4WS vehicle equipped with DYC [5] to improve the trajectory following of autonomous ground vehicles. He at al. propose robust coordination control of AFS and ARS based on H∞ controller [8]. The proposed algorithm shows improved path tracking and stability of autonomous vehicles. A combination of SMC controller with Luenberger observer is applied in [10] in 4WID-4WIS vehicle to allow improved trajectory following. SMC control for path following manoeuvres is applied in 4WID vehicle [2] and in 4WIS vehicles [13,19].

The purpose of this research is to improve the handling and the stability of an automated vehicle with integrated 4WIS and VSC system using Sliding Mode Control. The proposed control algorithm utilizes the advantages of the 4WIS system by combining AFS and ARS systems, while maintaining Ackerman steering geometry thus enhancing the vehicle handling. When the stability of the vehicle is critically endangered then the VSC system is activated to stabilize the vehicle. The proposed control algorithm is also effective in following a predefined path trajectory while traveling at lower and higher velocities. The open-loop manoeuvres are defined using the standard ISO 7401 [17], while the path following manoeuvres are inspired by the standard ISO 3888-1 [17]. The main contribution of this study is the application of SMC controllers in steer-by-wire vehicle equipped with 4WIS and VSC, where the proposed concept can be used in both open loop and path following manoeuvres. The 4WIS system allows improvement in vehicle handling and stability while the occasional involvement of the VSC system further improves the vehicle stability. The integrated control algorithm exploits the advantages of both systems.

1 VEHICLE MODELS

Three vehicle models are used in this research: 3D virtual model created in ADAMS/Car, linear bicycle model and nonlinear bicycle model. The 3D virtual model is used to represent the real vehicle and to test the proposed control algorithm, while the bicycle models are used as reference models and for defining and executing the control algorithm.

1.1 4WIS virtual vehicle model

The 4WIS virtual vehicle model is created in the ADAMS/Car software. It consists of 4 independent steering wheels actuated by linear actuators. Two of the actuators responsible for the same axle steering wheels are positioned in one shared housing, but they are actuated individually. A steering wheel is still positioned in the vehicle through which the driver controls the vehicle's direction, but there is no mechanical linkage between the steering wheel and the steered wheels, thus achieving steer-by-wire steering system. The tested vehicle is equipped with vehicle stability control system (VSC), active front steering (AFS) and active rear steering (ARS) systems. These systems are explained in detail in the next section and this vehicle would be referred as VSC + 4WIS vehicle (figure 1).

The vehicle model represents a large crossover SUV with mass of 2150 kg. The vehicle is equipped with nonlinear tire models based on the Magic tire formula (Pacejka model 2002) and front and rear MacPherson suspension system. The vehicle parameters are presented in table 1.

Additionally to the VSC + 4WIS vehicle, two 3D vehicle models with standard front wheel steering system are created. One vehicle is without any automated system (passive vehicle) and another vehicle equipped only with VSC system implemented, referred to as VSC vehicle. These vehicles were created in order to compare the vehicle with the 4WIS system with vehicles with conventional steering system.

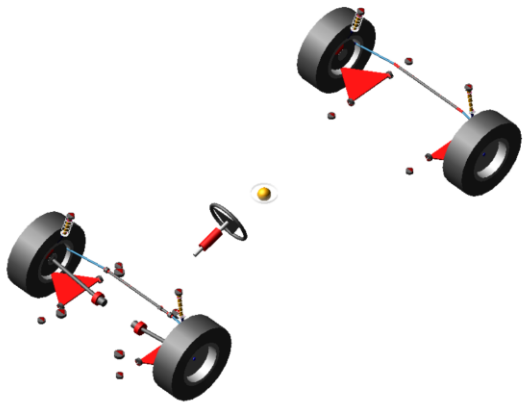

Figure 1 4WIS virtual vehicle model in ADAMS/CAR

Table 1 4WIS Virtual vehicle model - parameters

Mass (m):	2150 kg
Vehicle weight distribution (front/rear):	50/50 %
Length (L):	4635 mm
Width (W):	1890 mm
Wheelbase (l)::	3000 mm
Front track width (b_f):	1508 mm
Rear track width: (b_r):	1508 mm

1.2 Linear bicycle model

Next, 2DOF linear bicycle model (figure 2) with rear wheel steering is used for the SMC controllers of the 4WIS system. Linear bicycle model is used for a simpler control algorithm for the 4WIS system and faster computation. On the other hand, the 4WIS system is mostly capable of improving the handling and stability of the vehicle in the linear region of the tires, while in terms of stability, when the vehicle is near its limits, the tires are well in the nonlinear region. In this situation the 4WIS system can help in stabilization of the vehicle, but the vehicle stability control system is more dominant. The linear bicycle model is defined using equations (1) and (2).

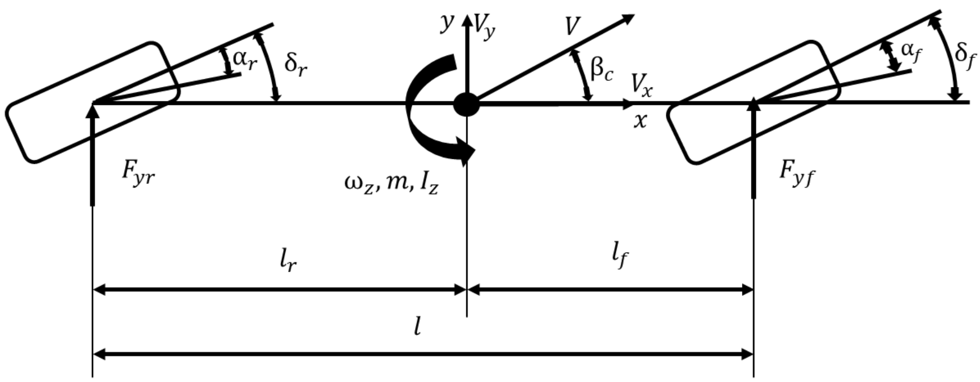

Figure 2 4WS Bicycle vehicle model

$$\dot{V}_y = \left(\frac{-C_{\alpha f}-C_{\alpha r}}{mV_x}\right)V_y + \left(\frac{C_{\alpha r}l_r-C_{\alpha f}l_f}{mV_x} - V_x\right)\omega_z + \frac{C_{\alpha f}}{m}\delta_f + \frac{C_{\alpha r}}{m}\delta_r, \tag{1}$$

$$\dot{\omega}_z = \left(\frac{C_{\alpha r}l_r-C_{\alpha f}l_f}{I_zV_x}\right)V_y + \left(\frac{-C_{\alpha f}{l_f}^2-C_{\alpha r}{l_r}^2}{I_zV_x}\right)\omega_z + \frac{C_{\alpha f}l_f}{I_z}\delta_f - \frac{C_{\alpha r}l_r}{I_z}\delta_r, \tag{2}$$

The bicycle model is defined by its lateral velocity V_y and yaw rate ω_z. I_z defines vehicle material moment of inertia, β_c - vehicle side-slip angle, l_f and l_r define the distance from center of mass to the front and rear axle respectively. The input variables to the system are the front wheel steering angle (δ_f) and the rear wheel steering angle (δ_r). During the co-simulation the longitudinal velocity (V_x) is not constant, rather it is fed to the linear bicycle model from the current velocity of the virtual vehicle model from ADAMS/Car. In equation (3) the state-space model of the bicycle model is presented. It is used in the control algorithms.

$$\begin{bmatrix}\dot{V}_y\\ \dot{\omega}_z\end{bmatrix} = \begin{bmatrix}a_{11}a_{12}\\ a_{21}a_{22}\end{bmatrix}\begin{bmatrix}V_y\\ \omega_z\end{bmatrix} + \begin{bmatrix}b_{11}\\ b_{21}\end{bmatrix}\delta_f + \begin{bmatrix}b_{12}\\ b_{22}\end{bmatrix}\delta_r, \tag{3}$$

where $a_{11} = \frac{-C_{\alpha f}-C_{\alpha r}}{mV_x}$, $a_{12} = \frac{C_{\alpha r}l_r-C_{\alpha f}l_f}{mV_x} - V_x$, $a_{21} = \frac{C_{\alpha r}l_r-C_{\alpha f}l_f}{I_zV_x}$, $a_{22} = \frac{-C_{\alpha f}{l_f}^2-C_{\alpha r}{l_r}^2}{I_zV_x}$, $b_{11} = \frac{C_{\alpha f}}{m}$, $b_{12} = \frac{C_{\alpha r}}{m}$, $b_{21} = \frac{C_{\alpha f}l_f}{I_z}$, $b_{22} = -\frac{C_{\alpha r}l_r}{I_z}$ while $C_{\alpha f}$ and $C_{\alpha r}$ represent the cornering stifness of the front and rear tires, respectively.

1.3 Nonlinear bicycle model

Beside the linear bicycle model, a nonlinear vehicle bicycle model is used in the proposed concept. A 2WS nonlinear bicycle model (figure 3) is used as a reference model for the passive and the VSC vehicle, while 4WS nonlinear reference bicycle model is used for the VSC+4WIS vehicle. The nonlinear bicycle model is described using equations (4) and (5). The same principle for the longitudinal velocity is applied here for the nonlinear bicycle model.

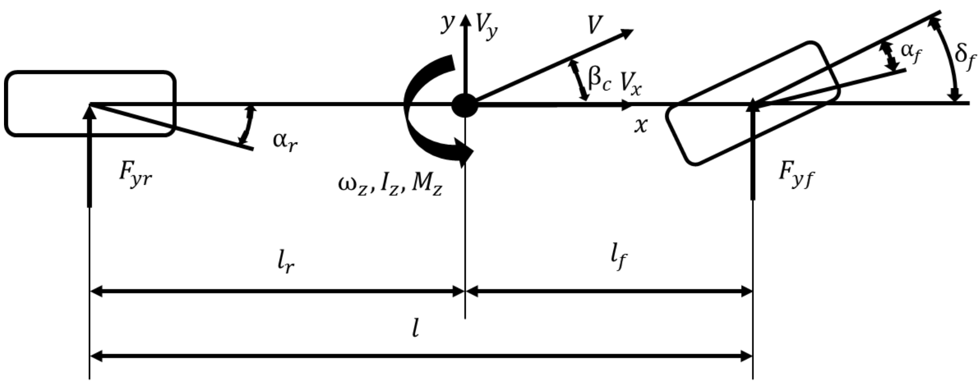

Figure 3 2WS Bicycle vehicle model

$$m(\dot{V}_y + V_x\omega_z) = F_{yf} + F_{yr}, \tag{4}$$

$$I_z\dot{\omega}_z = F_{yf}l_p - F_{yr}l_z, \tag{5}$$

The tire models are defined using the Magic Tire Formula presented in equations (6) and (7) where the front F_{yf} and rear F_{yr} tire lateral forces are defined in function to the front $\beta_f = \delta_f - \alpha_f$ and rear $\beta_r = \delta_r - \alpha_r$ tire side slip angles.

$$F_{yf} = D\sin\{C\text{atan}[B\beta_f - E(B\beta_f - \text{atan}(B\beta_f))]\}, \quad (6)$$

$$F_{yr} = D\sin\{C\text{atan}[B\beta_r - E(B\beta_r - \text{atan}(B\beta_r))]\}, \quad (7)$$

The coefficients of the Magic Tire Formula are presented in table 2 and are chosen for driving on a wet surface with μ=0.4. These conditions are chosen during the co-simulation in order to test the vehicle stability and handling.

Table 2 *Bicycle vehicle model and Magic Tire Formula - parameters*

Front tire cornering stiffness ($C_{\alpha f}$):	120000 N/rad
Rear tire cornering stiffness ($C_{\alpha r}$):	120000 N/rad
Inertia radius (i):	1275 mm
Pacejka tire model stiffness factor (*B*):	$C_{F\beta}/(CD)$
Pacejka tire model stiffness $C_{F\beta}$:	$C_a sin\left\{(2\, atan\left(\frac{F_n}{F_{nom}}\right)\right\}$
Pacejka tire model shape factor (*C*):	1.2
Pacejka tire model peak factor (*D*):	μF_n
Pacejka tire model curvature factor (*E*):	0

In table 2 the F_n parameter defines the tire vertical load. For the reference 4WS bicycle model, a linear control strategy is being used for the rear wheel steering. The control strategy is derived from equation (1) and it enables the vehicle to achieve zero value of the side-slip angle in steady and transient state. This reference model and control strategy presented in equation (8) is used because it had shown improved vehicle stability and handling in our previous research [1].

$$\delta_r = -\frac{C_{\alpha f}}{C_{\alpha r}}\delta_f + \frac{mV_x^2 + C_{\alpha f}l_f - C_{\alpha r}l_r}{C_{\alpha r}V_x}\omega_z, \quad (8)$$

2 PROPOSED CONTROL ALGORTIHM

The control strategy that is used in this research is based on sliding mode control theory. In equation (9) the sliding surface (s_i) is defined, where the error (e) is defined in equation (10) as a difference between the actual yaw rate (ω_z) of the 4WIS virtual model and the reference yaw rate (ω_{zref}).

$$s_i = \dot{e} + \lambda_i e \quad (9)$$

$$e = \omega_z - \omega_{zref} \quad (10)$$

To avoid destabilization of the refence model and thus destabilizing the 4WIS virtual vehicle, a limitation of the maximum yaw rate ω_{zmax} is defined using equation (11).

$$\omega_{zmax} = \left|\frac{\mu g}{V_x}\right| \quad (11)$$

The proposed control algorithm for the VSC+4WIS vehicle is presented in figure 4. The steering wheel angle applied by the driver is also used for the reference vehicle bicycle model where a steering ratio between the steering wheel and front steering wheels is assumed to be 1:16.71. A comparison between the actual yaw rate ω_z of the virtual vehicle model and the reference vehicle model ω_{zref} is made, thus defining the error (equation

(10)). The error signal is applied to the three SMC controllers. From here the 4WIS controllers output is applied to an Ackerman steering geometry to generate 4 independent steering angles, while the VSC controller output is applied to a torque distributor to generate 4 independent braking torques on each wheel. These elements and each SMC controllers are explained in detail in the next subsections.

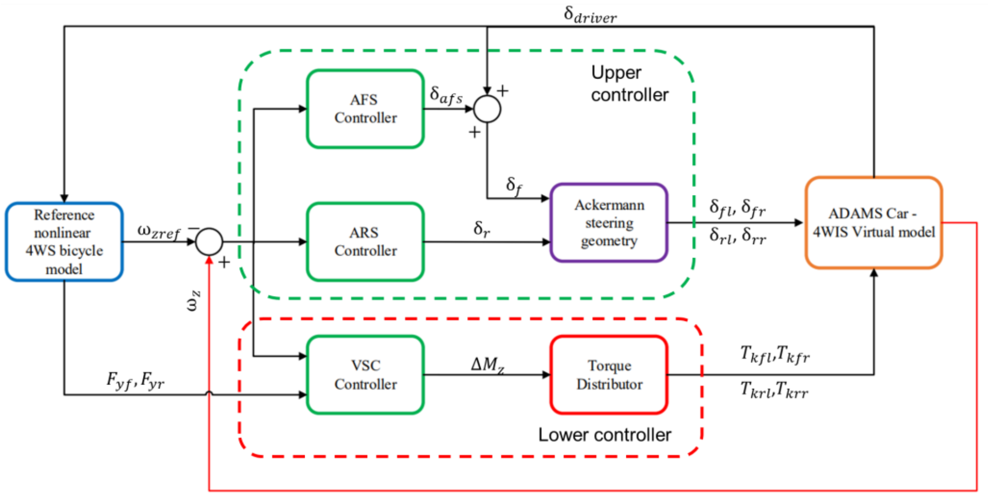

Figure 4 Proposed control algorithm diagram

2.1 4WIS control strategy

4WIS steering system control strategy is based on the linear bicycle model. As mentioned before this was adopted because the 4WIS system would have bigger impact on vehicle handling when the vehicle is not near its limits and is most effective in the linear region of the tires. Additionally, the usage of linear model allows faster computing process. The 4WIS control strategy is also named as upper controller in the system which is active continuously during the co-simulation. Although the vehicle possesses a steer-by-wire system, still the initial input to the system is defined by the driver and the steering wheel angle. The 4WIS control strategy is divided into two individual SMC controllers, one responsible for controlling the rear axle entirely and another responsible for correcting the driver's input to the front axle. In its core the 4WIS control strategy represents a combination of AFS and ARS systems.

The front wheels SMC controller is only responsible for correcting the driver's input and still the main command comes from the driver. Therefore, the front wheels steering angle is defined as combination of the driver's input (δ_{driver}) and the SMC controller output (δ_{afs}): $\delta_f = \delta_{driver} + \delta_{afs}$. If the desired error is $e = 0$, then the sliding surface would be $s = 0$. With that assumption if we combine equations (9) and (10), equation (12) is defined as:

$$\dot{e} = -\lambda_i e \tag{12}$$

By combining equation (2) and equation (12) the control law for the first SMC controller is presented in equation (13).

$$\delta_{afs} = \frac{1}{b_{21}}\left[-a_{21}V_y - a_{22}\omega_z - b_{21}\delta_{driver} - b_{22}\delta_r + \dot{\omega}_{ref} - \lambda_{afs}\left(\omega_z - \omega_{ref}\right)\right] \tag{13}$$

$$-k_{afs}tanh\left(\frac{s}{\phi_{afs}}\right)$$

where the controller parameters are $\lambda_{afs} = 3$ and $k_{afs} = 0.087$, while sliding surface thickness is $\phi_{afs} = 10$. The same principle is applied for the second SMC controller which is responsible for the independent steering angle of the rear wheels. In this case the SMC controller output defines the rear steering angle. The control law is presented in equation 14.

$$\delta_r = \frac{1}{b_{22}}\left[-a_{21}V_y - a_{22}\omega_z - b_{21}(\delta_{driver} + \delta_{afs}) + \dot{\omega}_{ref} - \lambda_{ars}\left(\omega_z - \omega_{ref}\right)\right] \\ -k_{ars}tanh\left(\frac{s}{\phi_{ars}}\right) \tag{14}$$

where $\lambda_{ars} = 3$, $\phi_{ars} = 10$ and $k_{ars} = 0.087$. Combining equation (13) and (14) the 4WIS control law is derived. These two SMC controllers are defined as coupled control laws. The reason that coupled control laws are used instead of uncoupled is to derive more precise steered wheels angles and to achieve improved vehicle handling. On the other hand, this will result in increased demand for computation power and longer duration of the co-simulation.

2.2 Ackerman steering geometry

The output of the 4WIS SMC controllers defines the desired front and rear steering angles of the vehicle bicycle model. To define the steering angles of the four wheels, an Ackerman steering geometry is used (figure 5). Depending on the front and rear wheels steering directions, two cases are defined. The first case is when the front and rear wheels are steered in same direction and the second case when the wheels are steered in opposite direction. Based on the SMC controller outputs and the desired steering angles, equations (15.a) and (15.b) are used when the SMC controllers impose same direction steering angles and equations (16.a) and (16.b) are used when the controllers demand opposite direction steering. δ_{fi} and δ_{fo} define the front inner and outer steering wheel angle respectively, while δ_{ri} and δ_{ro} define the rear inner and outer steering wheel angle respectively.

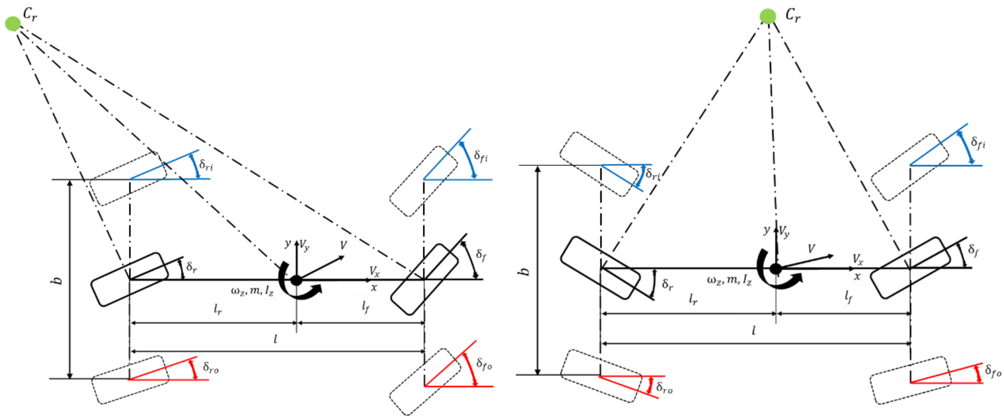

Figure 5 4WIS kinematic model, (a) Front and rear wheels are turned in the same direction, (b) Front and rear wheels are turned in the opposite direction.

$$\delta_{fi} = \text{atan}\left(\frac{\tan\delta_f}{1 - \frac{b}{2l}\left(\tan\delta_f - \tan\delta_r\right)}\right),\ \delta_{fo} = \text{atan}\left(\frac{\tan\delta_f}{1 + \frac{b}{2l}\left(\tan\delta_f - \tan\delta_r\right)}\right) \tag{15.a}$$

$$\delta_{ri} = \operatorname{atan}\left(\frac{\tan\delta_r}{1-\frac{b}{2l}\left(\tan\delta_f-\tan\delta_r\right)}\right),\ \delta_{ro} = \operatorname{atan}\left(\frac{\tan\delta_r}{1+\frac{b}{2l}\left(\tan\delta_f-\tan\delta_r\right)}\right) \tag{15.b}$$

$$\delta_{fi} = \operatorname{atan}\left(\frac{\tan\delta_f}{1-\frac{b}{2l}\left(\tan\delta_f+\tan\delta_r\right)}\right),\ \delta_{fo} = \operatorname{atan}\left(\frac{\tan\delta_f}{1+\frac{b}{2l}\left(\tan\delta_f+\tan\delta_r\right)}\right) \tag{16.a}$$

$$\delta_{ri} = \operatorname{atan}\left(\frac{\tan\delta_r}{1-\frac{b}{2l}\left(\tan\delta_f+\tan\delta_r\right)}\right),\ \delta_{ro} = \operatorname{atan}\left(\frac{\tan\delta_r}{1+\frac{b}{2l}\left(\tan\delta_f+\tan\delta_r\right)}\right) \tag{16.b}$$

2.3 *VSC control strategy*

Unlike the 4WIS control strategy a SMC controller algorithm for the VSC system is derived based on a nonlinear vehicle bicycle model. This is because the VSC system is activated when the tires are in their nonlinear region and the vehicle is on verge of destabilization. To define the VSC controller in equation (5) the corrective yaw moment ΔM_z is added. In this case the vehicle bicycle model is presented in figure 6 with the corrective yaw moment ΔM_z and the new equation is presented in equation (17). Using the same analogy as the 4WIS controllers and equations (12) and (17), the VSC controller output is defined using the equation (18).

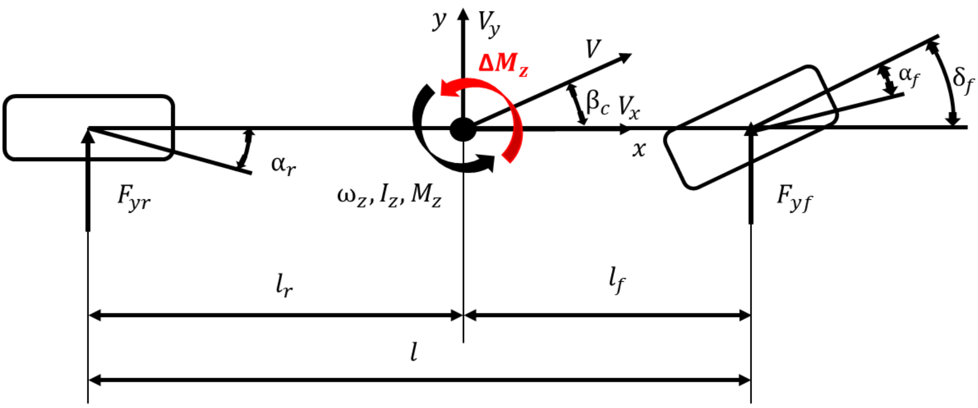

Figure 6 2WS Bicycle vehicle model with corrective yaw moment

$$I_z\dot{\omega}_z = F_{yf}l_p - F_{yr}l_z + \Delta M_z \tag{17}$$

$$\Delta M_z = -F_{yf}l_p + F_{yr}l_z - I_z\dot{\omega}_{ref} + I_z\lambda_{vsc}\left(\omega_z-\omega_{ref}\right) - k_{vsc}tanh\left(\frac{s}{\phi_{vsc}}\right) \tag{18}$$

where $\lambda_{vsc} = 3$, $\phi_{vsc} = 3$ and $k_{vsc} = -3$. After defining the desired corrective yaw moment form the SMC controller, a braking torque distribution must be made to each wheel. The VSC system is designed to brake the wheels on same side simultaneously. If the value $\Delta M_z > 0$ then the left wheels are braked, while when $\Delta M_z < 0$ the right wheels are braked. The braking forces of each wheel in relation with the ΔM_z are presented in equation (19).

$$\Delta M_z = \frac{F_{xfl} b_f}{2} + \frac{F_{xrl} b_r}{2} - \frac{F_{xfr} b_f}{2} - \frac{F_{xrr} b_r}{2} \tag{19}$$

where F_{xij} defines the longitudinal tire force on each wheel while b_f and b_f represent vehicle front and rear track width respectively. Using equation (20) the total braking torque that should be applied to wheels is taken into consideration.

$$\begin{cases} \Delta M_z > 0 \rightarrow \quad Tk = (F_{xfl} + F_{xrl}) r_d \\ \Delta M_z < 0 \rightarrow \quad Tk = (F_{xfr} + F_{xrr}) r_d \end{cases} \tag{20}$$

where $r_d = 0.33\ m$ represents the tires rolling radius and the braking system is designed to allow 60/40 torque distribution between the front and rear wheels.

To avoid constant activation of the VSC system a phase-plane method $(\beta - \dot{\beta})$ is used. The stable region is bellow the value of 0.7 which is determined by testing the proposed control algorithm. This value allows activation of the VSC system to stabilize, but also the activation is not so frequent thus allowing the vehicle to perform different manoeuvres without interference in the stable region of the phase-plane method $(\beta - \dot{\beta})$.

$$\left| \mathrm{C}_1 \beta + \mathrm{C}_2 \dot{\beta} \right| \leq 0.7 \tag{19}$$

The values of $\mathrm{C}_1 = 2.41$ and $\mathrm{C}_2 = 9.615$ are used as suggested in [9].

2.4 4WIS control strategy for path following manoeuvres

For the path following manoeuvres a modification of the 4WIS must be made. In this case the driver is omitted and there is no input from him while the vehicle is forced to follow predefined trajectory. Therefore, the reference variables are now changed and the sliding surface and error are defined differently. Instead of the yaw rate error (equation (10)) the path deviation is defined using the lateral position y and yaw angle φ of the vehicle. The new error e_p is defined in equation (20) by combination of lateral position error $e_1 = y - y_{ref}$ and yaw angle error $e_2 = \varphi - \varphi_{ref}$.

$$e_p = y - y_{ref} + \xi(\varphi - \varphi_{ref}) \tag{20}$$

where $\xi = 1.5$ represents a weighing coefficient. The reference lateral position y_{ref} is preditermied based on the defined trajectory while the reference yaw angle φ_{ref} is defined in equation (21) [13] based on the relations described by Rajamani [14].

$$\varphi_{ref} = \mathrm{atan} \frac{\dot{y}_{ref}}{\dot{x}_{ref}} \approx \frac{\dot{y}_{ref}}{\dot{x}_{ref}} \tag{21}$$

From here the error derivative is described using equation (22).

$$\dot{e}_p = V_x \varphi + V_y - \dot{y}_{ref} + \xi(w_z - \dot{\varphi}_{ref}) \tag{22}$$

After combining the equations (1), (2) and (12) with equations (20), (21) and (22) the coupled control laws for the front δ_{fp} and rear δ_{rp}wheel angles for path following are defined using equations (23) and (24).

$$\delta_{fp} = \frac{1}{b_{11}} \left[a_{11} V_x \varphi + \dot{V}_y - a_{12} \omega_z - b_{12} \delta_{rp} + \dot{y}_{ref} + \xi \left(w_z - \dot{\varphi}_{ref} \right) + \right. \tag{23}$$

$$\lambda_{fp}(e_1 + \xi e_2)\big] - k_{fp} tanh\left(\frac{s}{\phi_{fp}}\right)$$

$$\delta_{rp} = \frac{1}{b_{12}}\big[a_{11}V_x\varphi + \dot{V}_y - a_{12}\omega_z - b_{11}\delta_{fp} + \dot{y}_{ref} + \xi(w_z - \dot{\varphi}_{ref}) + \lambda_{rp}(e_1 + \xi e_2)\big] - k_{rp} tanh\left(\frac{s}{\phi_{rp}}\right) \tag{24}$$

where $\lambda_{fp} = \lambda_{rp} = 3$, $\phi_{fp} = \phi_{rp} = 10$ and $k_{fp} = k_{rp} = 0.087$. The proposed control law is presented in figure 7, where it can be observed that the control law for the VSC system remains the same where a yaw rate error is used for system control, while the reference yaw rate is still obtained from the nonlinear bicycle model.

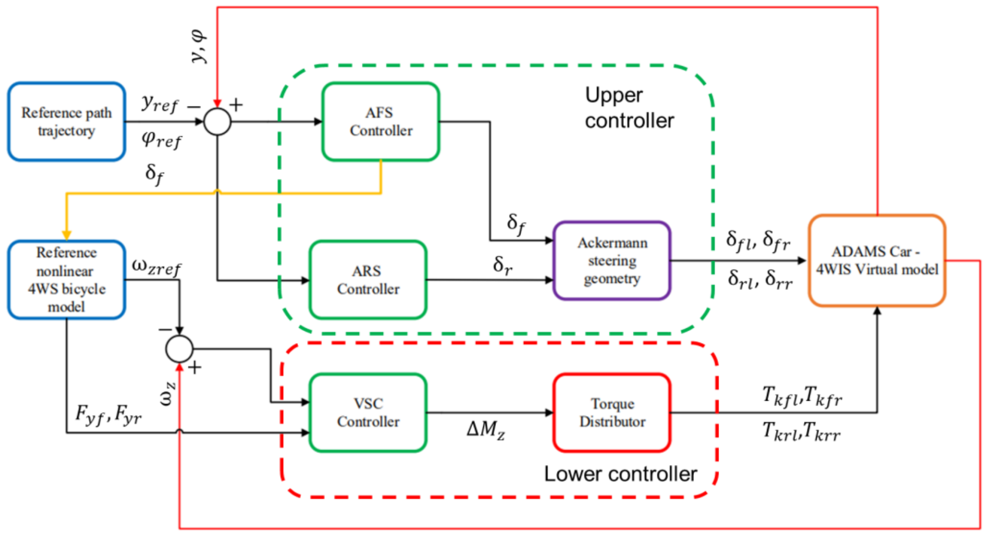

Figure 7 Proposed control algorithm diagram for path following manoeuvres

3 CO-SIMULATION RESULTS

To test the proposed control algorithm and the 4WIS steering system, a co-simulation was conducted where the virtual vehicles are tested using standardized open-loop and path following manoeuvres. The open-loop manoeuvres that were conducted are step-steer and single lane-change manoeuvre, based on the ISO 7401 standard with the vehicle travelling at 80 km/h. The velocity is not maintained during the manoeuvres, rather it decreases because of the activation of the VSC system or the destabilization of the vehicle. The open-loop manoeuvres are conducted on a wet surface with friction coefficient of μ=0.4. This surface was chosen in order to test the vehicles stability and handling in worsening road conditions and to achieve lateral acceleration of *4 m/s²* in order to fulfil the ISO 7401 standard.

3.1 Step-steer manoeuvre

According to the ISO 7401 standard, the steering wheel is turned for 0.5 s and is maintained at the maximum value during the manoeuvre. The maximum value of the steering wheel (figure 8) is determined as to achieve lateral acceleration of *4 m/s²* in steady-state condition (figure 9). Based on the analysis in figures 10 and 11 it could be observed that the

VSC+4WIS vehicle steers the wheels in same direction and the values of the front steering wheels angles are larger than the passive and VSC vehicle. That would impose the need for slightly larger mounting space for the steering system. Figure 9 shows that the standard ISO 7401 has been fulfilled and all vehicles achieve *4 m/s²* in steady-state condition. Also, all vehicles are at their physical limits. This can be also shown in figure 12 where the yaw rate of the passive vehicle indicates that the vehicle has started to lose its stability. On the other hand, both VSC and VSC+4WIS vehicles remain stable. This can be seen in figure 13 where the side-slip angle of the passive vehicle starts to rise exponentially. On the other hand, the VSC+4WIS vehicle has a near zero value of the side-slip angle, thus significantly improving the driver's awareness of the vehicle traveling direction. VSC+4WIS vehicle also shows lowest velocity decrease, while completing the manoeuvre successfully (figure 14). Figure 15 presents the trajectory of all the vehicles, and they are very similar. If the simulation time is prolonged, than a destabilization of the passive vehicle would be also shown on the trajectory diagram. It is also worth noting that the VSC system activates only the left wheel brakes (the vehicle turns to the left) indicating that the vehicles had shown understeer characteristics, but the activation of the brakes in VSC+4WIS vehicle is shorter (figure 16).

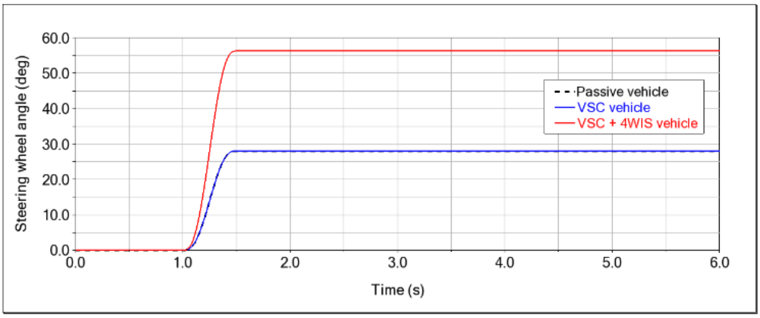

Figure 8 Steering wheel angle

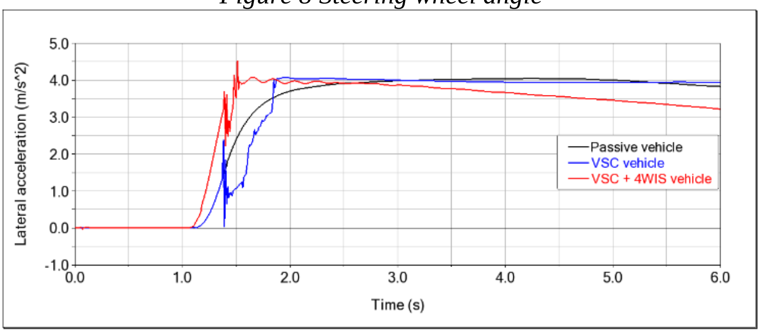

Figure 9 Lateral acceleration

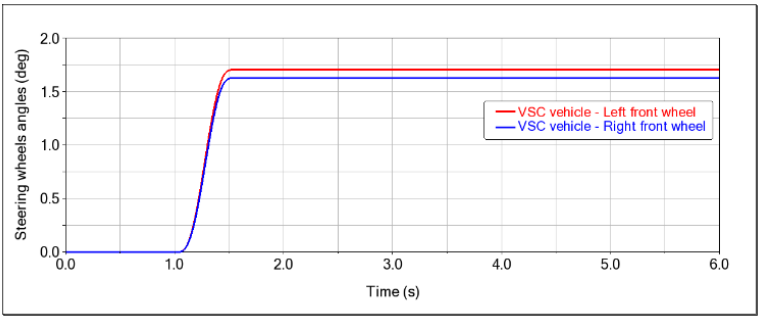

Figure 10 VSC vehicle - front and rear steering wheels angle

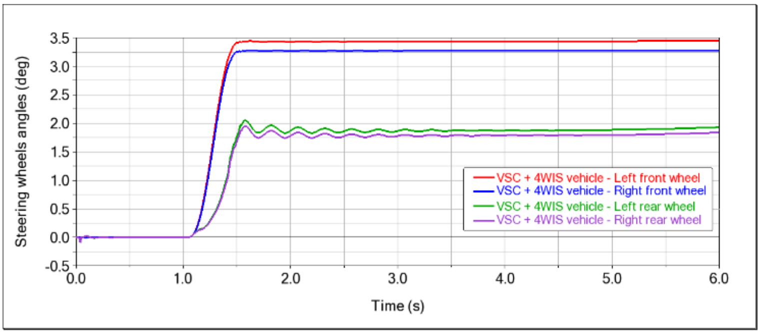

Figure 11 VSC + 4WIS vehicle - front and rear steering wheels angle

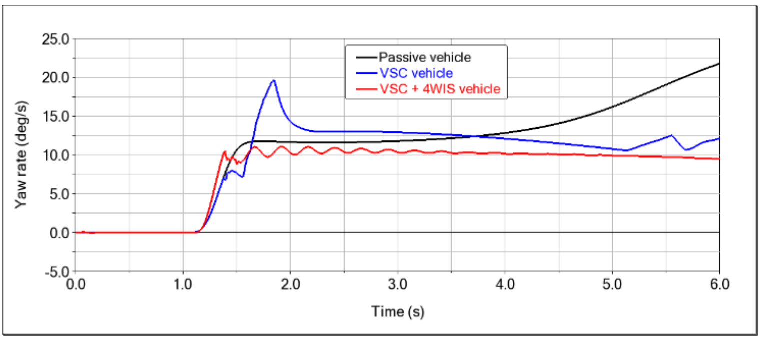

Figure 12 Yaw rate

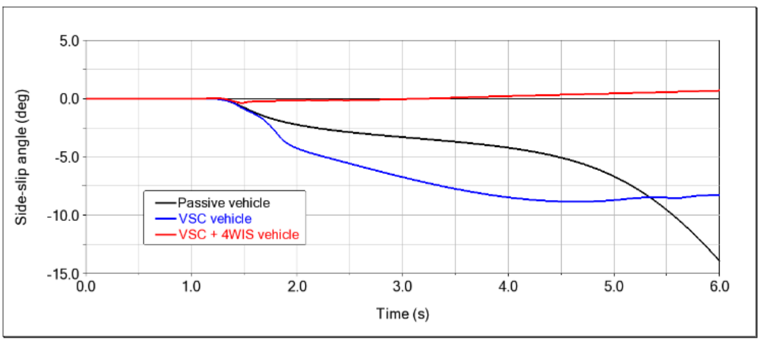

Figure 13 Side-slip angle

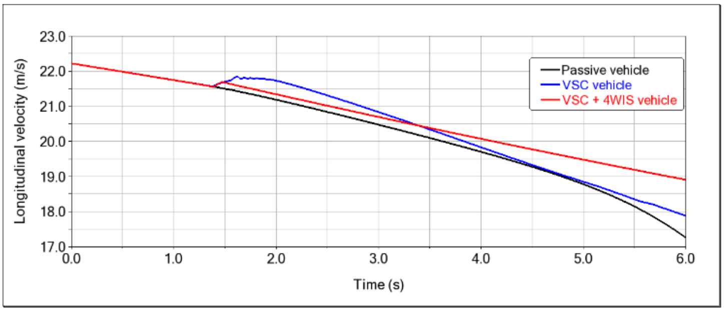

Figure 14 Longitudinal velocity

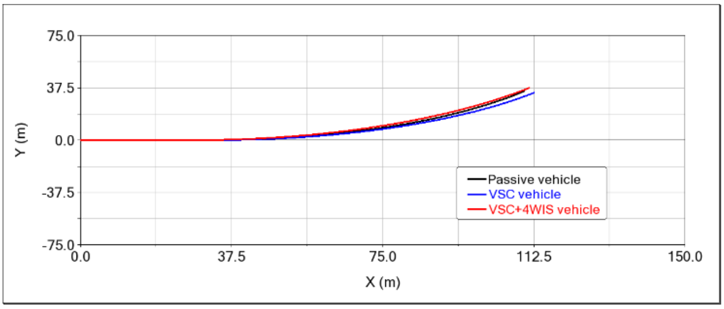

Figure 15 Trajectories

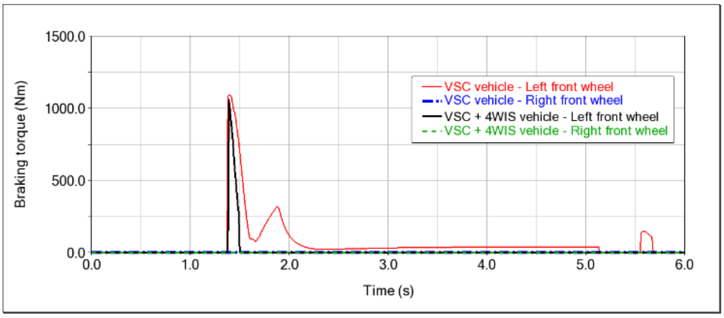

Figure 16 Braking torque – VSC and VSC + 4WIS vehicle

3.2 Single lane-change manoeuvre

Beside the step-steer manoeuvre, a single lane-change manoeuvre was conducted. The input signal form the driver is defined as one full period sinus function with frequency of 0.5 Hz (figure 17). According to the standard, the initial velocity of the vehicles is 80 km/h and the steering wheel angles are determined by the request for the vehicles to achieve lateral acceleration of $4\ m/s^2$ in the first peak value (figure 18). The conclusions are similar to the previous manoeuvre, but in this scenario the difference between the vehicles is larger. Figures 19 and 20 represents the steering wheel angles where the VSC+4WIS vehicle requires larger values. The first considerable difference could be observed in figure 18 where the passive vehicle loses its stability and fails to complete the manoeuvre. Also, the reaction time and the settling time of the VSC+4WIS vehicle is shorter than the VSC vehicle. The same conclusions can be derived from figure 21. The smoother transition of

VSC+4WIS and shorter settling time implies that the VSC+4WIS vehicle possesses improved handling and stability. This conclusion can be confirmed in figures 22 and 23 where the values of the side-slip angle of the VSC+4WIS are more than 2.5 times smaller than the VSC vehicle. In figures 22 and 25 it is once again shown that the passive vehicle loses its stability. Figure 25 also shows that the VSC+4WIS needs narrower road to complete the manoeuvre. During the manoeuvring of the vehicles with automated system, their velocity is decreased insignificantly compared to the passive vehicle that swerves out (figure 24). The superiority of the 4WIS system is more noticeable in this manoeuvre where the 4WIS manages to stabilize the vehicle while the VSC system is activated only in short time interval and with smaller braking torque values (figure. 26). On the other hand, the VSC system of the VSC vehicle is activated more often and with bigger intensity, but still the VSC vehicle shows reduced stability and handling characteristics compared to the VSC+4WIS vehicle.

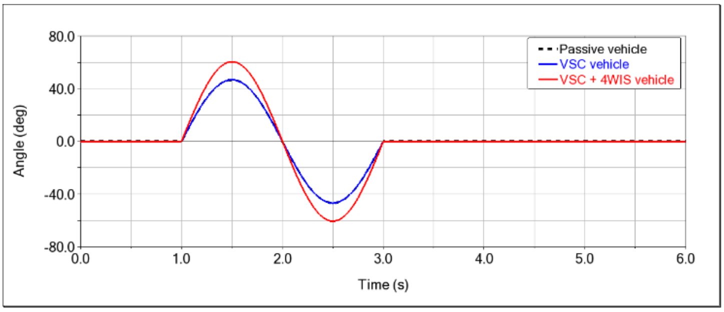

Figure 17 Steering wheel angle

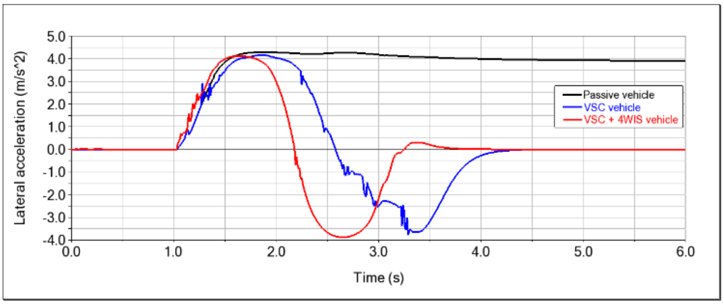

Figure 18 Lateral acceleration

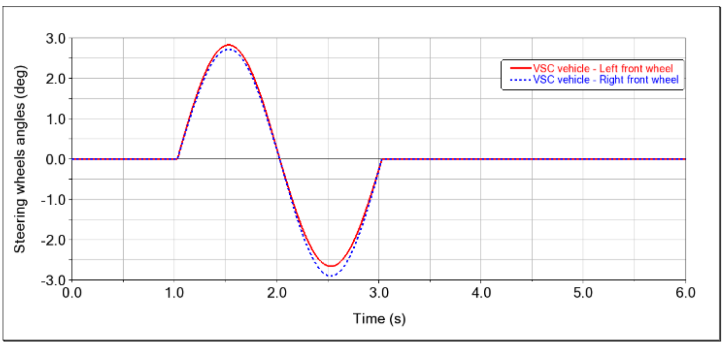

Figure 19 VSC vehicle - front and rear steering wheels angle

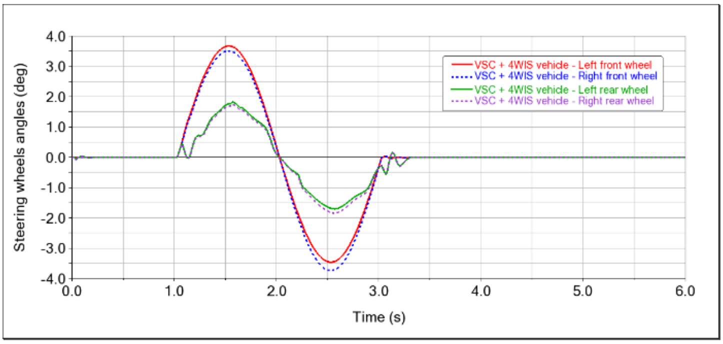

Figure 20 VSC + 4WIS vehicle - front and rear steering wheels angle

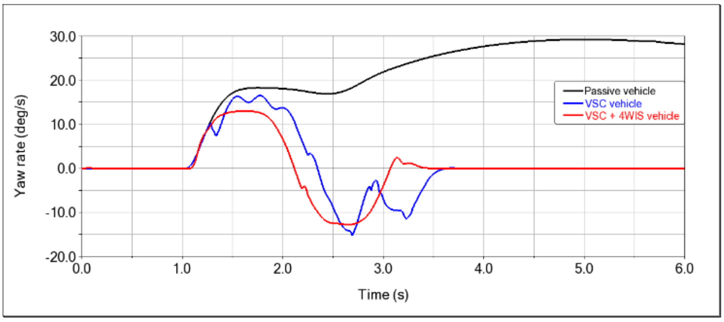

Figure 21 Yaw rate

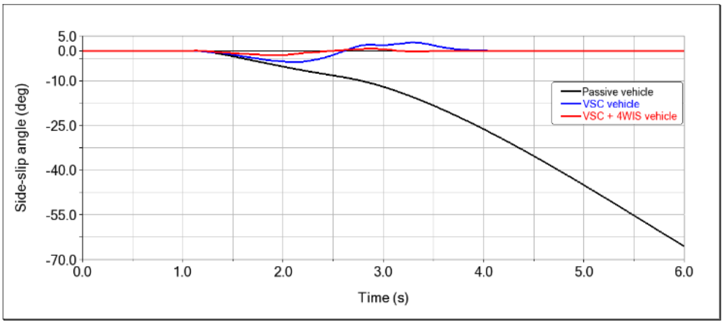

Figure 22 Side-slip angle

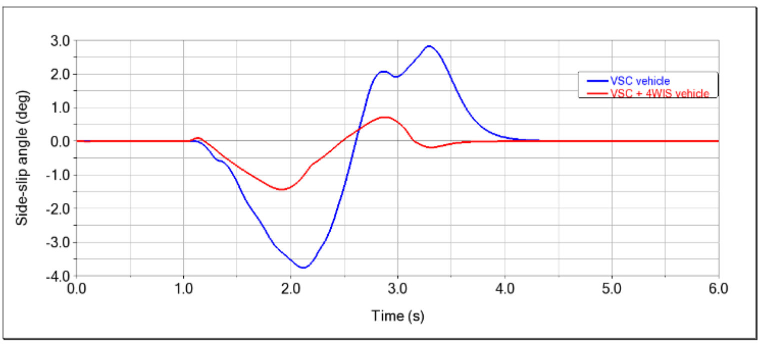

Figure 23 Side-slip angle of the alternative vehicles

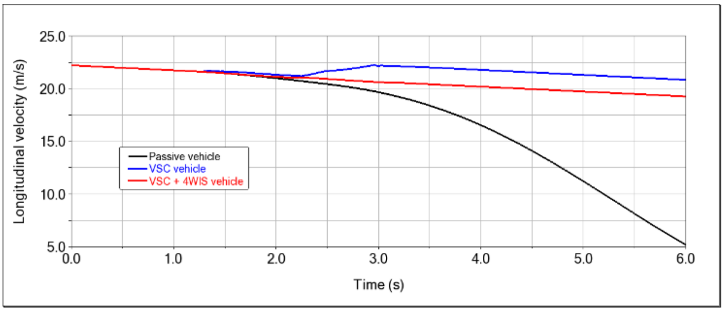

Figure 24 Longitudinal velocity

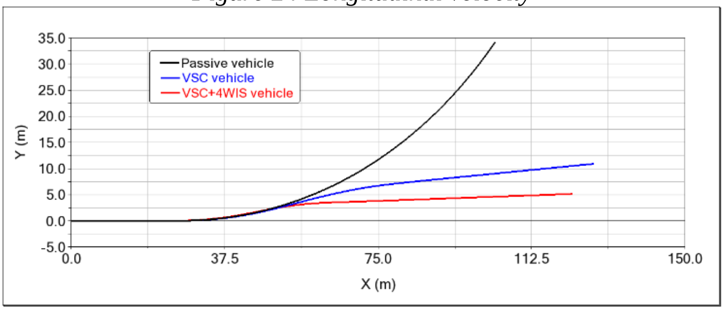

Figure 25 Trajectories

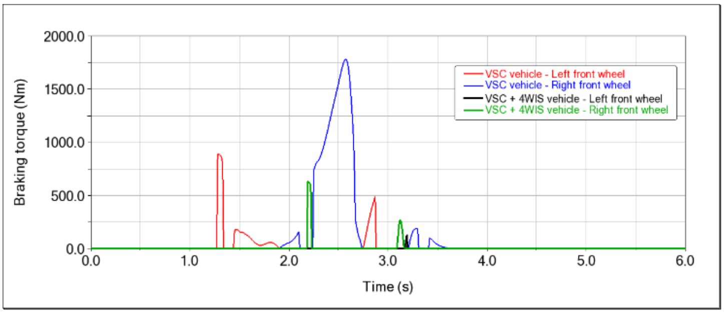

Figure 26 Braking torque – VSC and VSC + 4WIS vehicle

3.3 Path-following manoeuvres

The path-following manoeuvres are inspired by the ISO 3888 standard [16] where the trajectory dimensions and it's boundaries are defined according to it. The trajectory's boundaries are presented in figure 27, where the blue line represents the reference central line that the vehicle should follow. In order to make the trajectory smother, a combination of step and cosine function is defined These manoeuvres are conducted in order to test the proposed control algorithm of the VSC+4WIS vehicle and its capabilities to follow a desired trajectory. The co-simulation is conducted only on the VSC+4WIS vehicle because the other vehicles do not possess automated steering system. One simulation is performed where the vehicle is traveling at 50 km/h, a city cruising speed, and one simulation is conducted according to the standard where the vehicle is traveling at 80 km/h. The tests are conducted on dry surface with friction coefficient μ=0.9.

The first set of results represents a co-simulation when the vehicle is traveling with 50 km/h. In figure 27 it could be observed that the vehicle is following the reference trajectory within the boundaries of the vehicles. The offset of the reference trajectory can be result on several parameters such as the fact that the reference trajectory is purely kinematic and could be further optimized, the inertia of the vehicle itself, lack of longitudinal controller and lack of prediction horizon. Figure 28 shows the steering wheel angles, while from figures 29, 30 and 31 it can be concluded that the vehicle is stable during the manoeuvring process and the values are within the desired limits. Figure 32 presents the longitudinal velocity of the vehicle where it can be seen that the vehicle completes the manoeuvre successfully with the predefined velocity. Beside the 4WIS, the activation of the VSC system maintains the stability of the vehicle (figure 33).

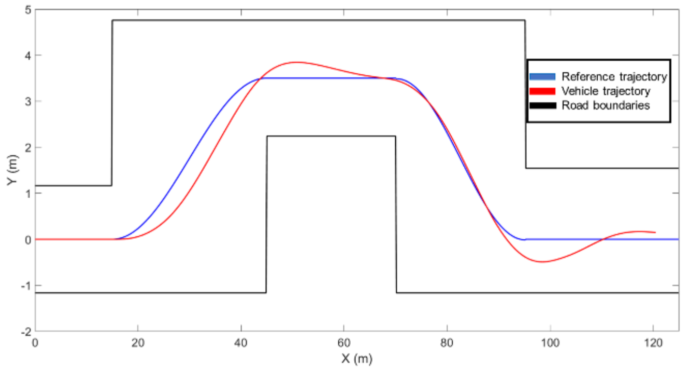

Figure 27 Trajectory – 50 km/h

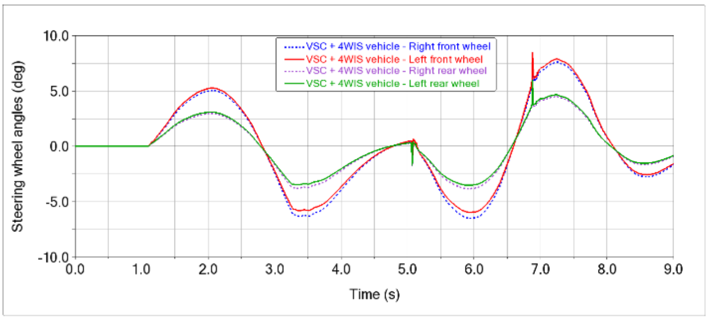

Figure 28 Front and rear steering wheels angle– 50 km/h

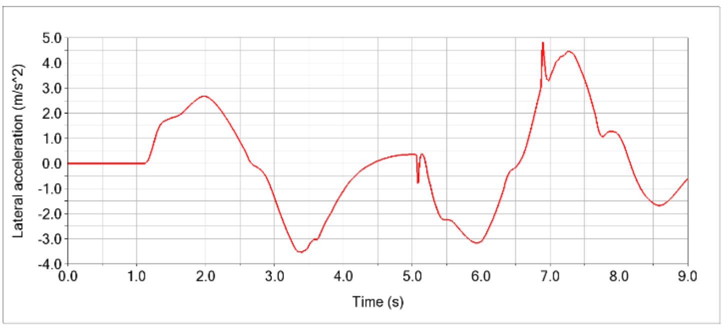

Figure 29 Lateral acceleration – 50 km/h

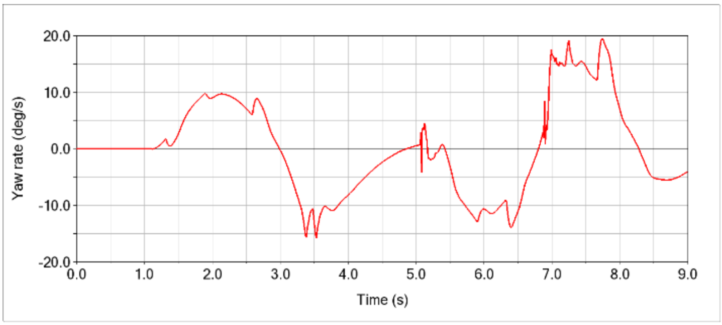

Figure 30 Yaw rate – 50 km/h

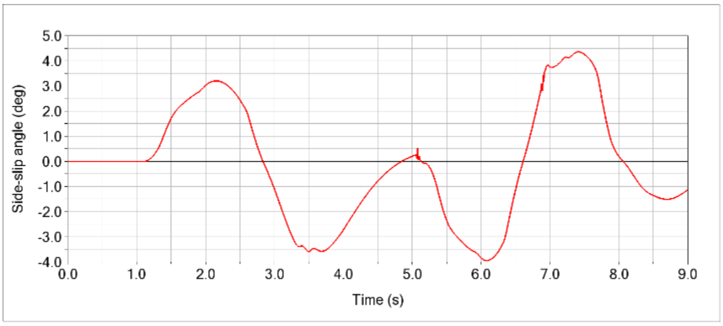

Figure 31 Side-slip angle – 50 km/h

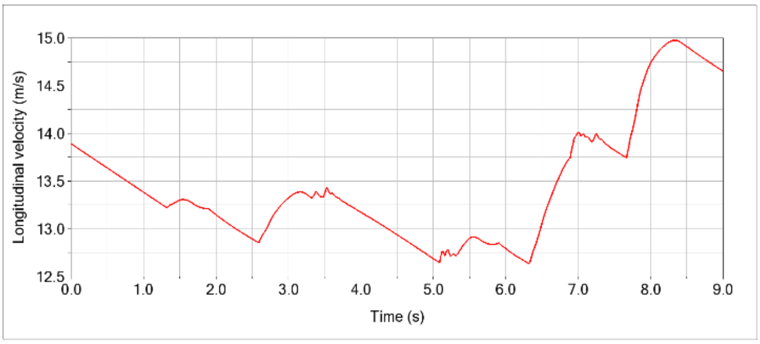

Figure 32 Longitudinal velocity – 50 km/h

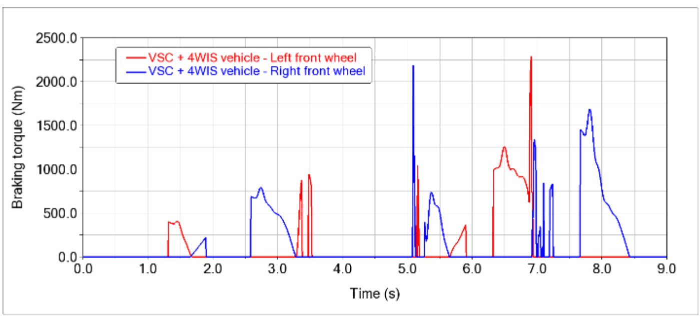

Figure 33 Braking torque –50 km/h

In order to test path-following capability of the proposed control algorithm of the VSC+4WIS vehicle the manoeuvre was repeated in a scenario where the vehicle is traveling at 80 km/h. From figure 34 it can be concluded that the vehicle passes the manoeuvre successfully, while maintaining its stability, at 60 meters longitudinally the vehicle shows larger offset of the reference trajectory. This may lead to small collision between the side of the vehicle and the road boundary. Figure 35 presents the steering wheel angle. Figures 36, 37 and 38 present the lateral acceleration, yaw rate and the side-slip angle where it can be observed that the vehicle maintains its stability, but due to the larger values compared to the previous manoeuvre it is obvious that the vehicle is on its limits. This could be also observed in figure 40 where the VSC system is activated more frequently and with higher intensity. During the manoeuvre the vehicle almost maintains the desired velocity (figure 39).

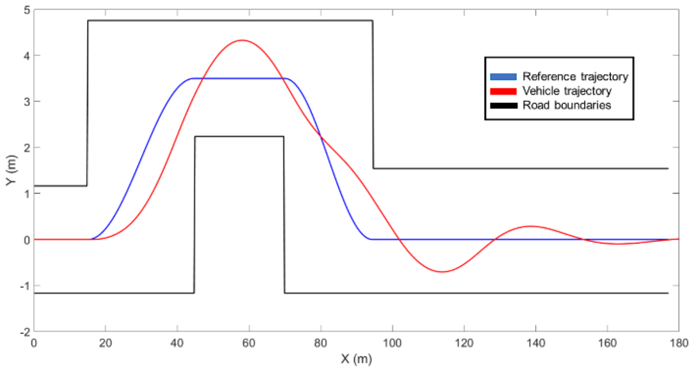

Figure 34 Trajectory – 80 km/h

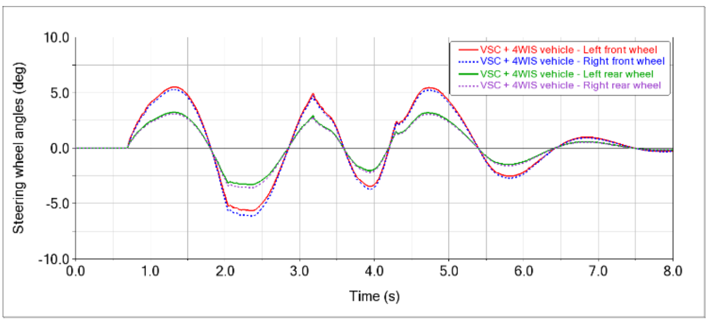

Figure 35 Front and rear steering wheels angle – 80 km/h

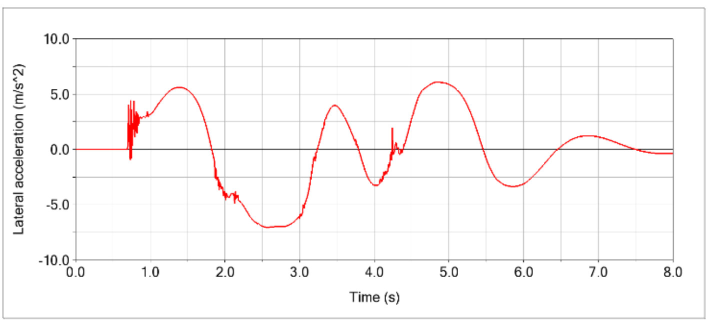

Figure 36 Lateral acceleration – 80 km/h

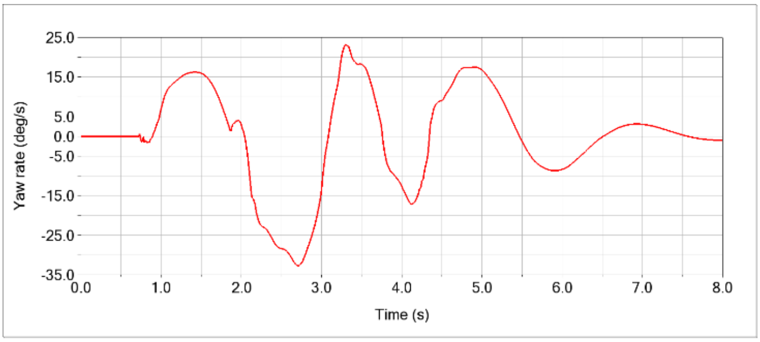

Figure 37 Yaw rate – 80 km/h

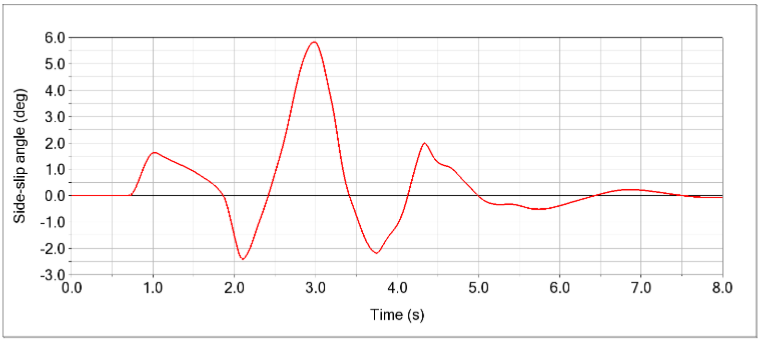

Figure 38 Side-slip angle – 80 km/h

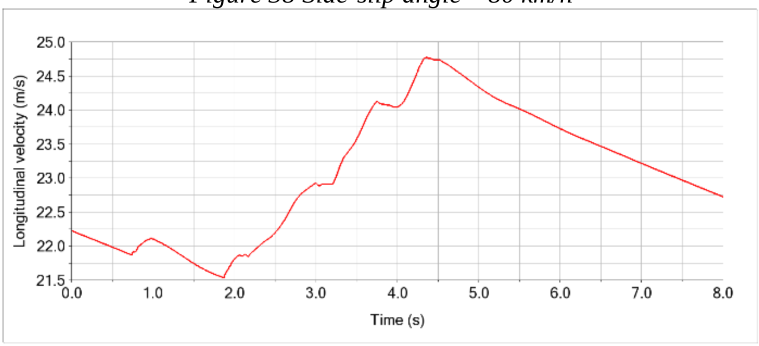

Figure 39 Longitudinal velocity– 80 km/h

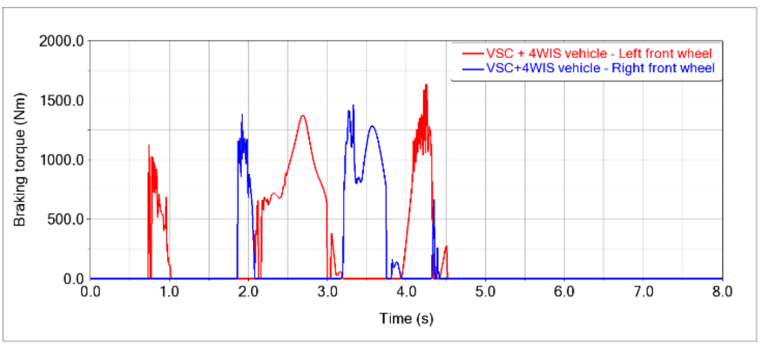

Figure 40 Braking torque – 80 km/h

4 CONCLUSIONS

The implementation of 4WIS steering system as a steer-by-wire system would improve the vehicle handling and stability of the vehicle as shown in this research. The VSC+4WIS has shown that the 4WIS system is responsible for improving vehicle handling and stability while the tires are in their linear region, but when combined with the VSC system the vehicle has improved stability in the tires nonlinear region. This can be confirmed with the fact that the VSC system is activated less frequently and with smaller intensity compared to the VSC vehicle. Also, lower vehicle side-slip angle values of the VSC+4WIS result in improved drivers handling feel during manoeuvring.

Beside the open loop manoeuvres, the proposed control algorithm with small modification could be implemented in path-following manoeuvre resulting in improved autonomous vehicle handling and stability. Further improvement in the control algorithm could be applied by adding longitudinal controller which would mostly improve the vehicle path-following capabilities.

REFERENCES

[1] Changoski, V., Gjurkov, I., Jordanoska, V.: "Improving vehicle dynamics employing individual and coordinated sliding mode control in vehicle stability, active front wheel steering and active rear wheel steering systems in co-simulation environment", In IOP Conference Series: Materials Science and Engineering, Vol. 1271, No. 1, 2022, p. 012026.

[2] Chen, J., Shuai, Z., Zhang, H., Zhao, W.: "Path following control of autonomous four-wheel-independent-drive electric vehicles via second-order sliding mode and nonlinear disturbance observer techniques", IEEE Transactions on Industrial Electronics, Vol. 68, No. 3, 2020, pp.2460-2469.

[3] Chen, X., Han, Y., Hang, P.: "Researches on 4WIS-4WID stability with LQR coordinated 4WS and DYC", In The IAVSD International Symposium on Dynamics of Vehicles on Roads and Tracks, 2019, pp. 1508-1516.

[4] Chen, X., Luo, F., Hang, P. Luo, J.: "Steering Mode Switch Control of Four-Wheel-Independent-Steering Electric Vehicle", In Proceedings of the 19th Asia Pacific Automotive Engineering Conference & SAE-China Congress 2017: Selected Papers, 2019, pp. 437-453.

[5] Hang, P., Chen, X., Luo, F.: "LPV/H∞ controller design for path tracking of autonomous ground vehicles through four-wheel steering and direct yaw-moment control", International Journal of Automotive Technology, Vol. 20, 2019, pp.679-691.

[6] Hang, P., Luo, F., Fang, S., Chen, X.: "Path tracking control of a four-wheel-independent-steering electric vehicle based on model predictive control", In 2017 36th Chinese control conference (CCC), 2017, pp. 9360-9366.

[7] Hang, P., Xia, X., Chen, X.: "Handling stability advancement with 4WS and DYC coordinated control: A gain-scheduled robust control approach", IEEE Transactions on Vehicular Technology, Vol. 70, No. 4, 2021, pp.3164-3174.

[8] He, X., Liu, Y., Yang, K., Wu, J., Ji, X.: "Robust coordination control of AFS and ARS for autonomous vehicle path tracking and stability", In 2018 IEEE International Conference on Mechatronics and Automation (ICMA), 2018, pp. 924-929.

[9] Jin, L., Xie, X., Shen, C., Wang, F., Wang, F., Ji, S., Guan, X., Xu, J.: "Study on electronic stability program control strategy based on the fuzzy logical and genetic

optimization method", Advances in Mechanical Engineering, Vol. 9, No. 5, 2017, p.1687814017699351.

[10] Lei, Y.L., Wen, G., Fu, Y., Li, X., Hou, B., Geng, X.: "Trajectory-following of a 4WID-4WIS vehicle via feedforward–backstepping sliding-mode control", Proceedings of the Institution of Mechanical Engineers, Part D: Journal of Automobile Engineering, Vol. 236, No. 2-3, 2022, pp.322-333.

[11] Liang, Y., Li, Y., Yu, Y., Zheng, L.: "Integrated lateral control for 4WID/4WIS vehicle in high-speed condition considering the magnitude of steering", Vehicle System Dynamics, Vol. 58, No. 11, 2020, pp.1711-1735.

[12] Mousavinejad, E., Han, Q.L., Yang, F., Zhu, Y., Vlacic, L.: "Integrated control of ground vehicles dynamics via advanced terminal sliding mode control", Vehicle System Dynamics, Vol. 55, No. 2, 2017, pp.268-294.

[13] Norouzi, A., Adibi-Asl, H., Kazemi, R. Hafshejani, P.F.: "Adaptive sliding mode control of a four-wheel-steering autonomous vehicle with uncertainty using parallel orientation and position control", International Journal of Heavy Vehicle Systems, Vol. 27, No. 4, 2020, pp.499-518.

[14] Rajamani, R.: "Vehicle dynamics and control", Springer Science & Business Media, 2011.

[15] Shuai, Z., Zhang, H., Wang, J., Li, J., Ouyang, M.: "Combined AFS and DYC control of four-wheel-independent-drive electric vehicles over CAN network with time-varying delays", IEEE Transactions on vehicular technology, Vol. 63, No. 2, pp.2013, 591-602.

[16] Standard ISO 3888-1:2018 - https://www.iso.org/standard/67973.html

[17] Standard ISO 7401:2011 https://www.iso.org/standard/54144.html 1

[18] UN Regulation No. 79 - https://unece.org/transport/documents/2023/10/working-documents/un-regulation-no-79-revision-5

[19] Wang, R., Yin, G., Jin, X.: "Robust adaptive sliding mode control for nonlinear four-wheel steering autonomous Vehicles path tracking systems", In 2016 IEEE 8th international power electronics and motion control conference (IPEMC-ECCE Asia), 2016, pp. 2999-3006.

[20] Yim, S., Jo, Y.H.: "Integrated chassis control with AFS, ARS and ESC under lateral force constraint on AFS", JMST Advances, Vol.1, 2019, pp.13-21.

[21] Zhang, J., Wang, H., Ma, M., Yu, M., Yazdani, A., Chen, L.: "Active front steering-based electronic stability control for steer-by-wire vehicles via terminal sliding mode and extreme learning machine", IEEE Transactions on Vehicular Technology, Vol. 69, No. 12, 2020, pp.14713-14726.

[22] Zheng, B., Anwar, S.: "Yaw stability control of a steer-by-wire equipped vehicle via active front wheel steering." Mechatronics, Vol. 19, No. 6, 2009, pp.799-804.